1521-0111/87/3/410–420$25.00
MOLECULAR PHARMACOLOGY

http://dx.doi.org/10.1124/mol.114.095133
Mol Pharmacol 87:410–420, March 2015

Engineering High-Potency R-spondin Adult Stem Cell Growth Factors[S]

Margaret L. Warner, Tufica Bell, and Augen A. Pioszak

Department of Biochemistry and Molecular Biology, The University of Oklahoma Health Sciences Center, Oklahoma City, Oklahoma

Received July 31, 2014; accepted December 12, 2014

ABSTRACT

Secreted R-spondin proteins (RSPOs1–4) function as adult stem cell growth factors by potentiating Wnt signaling. Simultaneous binding of distinct regions of the RSPO Fu1–Fu2 domain module to the extracellular domains (ECDs) of the LGR4 G protein–coupled receptor and the ZNRF3 transmembrane E3 ubiquitin ligase regulates Wnt receptor availability. Here, we examine the molecular basis for the differing signaling strengths of RSPOs1–4 using purified RSPO Fu1–Fu2, LGR4 ECD, and ZNRF3 ECD proteins in Wnt signaling and receptor binding assays, and we engineer novel high-potency RSPOs. RSPO2/3/4 had similar signaling potencies that were stronger than that of RSPO1, whereas RSPO1/2/3 had similar efficacies that were greater than that of RSPO4. The RSPOs bound LGR4 with affinity rank order RSPO4 > RSPO2/3 > RSPO1 and ZNRF3 with affinity rank order RSPO2/3 > > RSPO1 > RSPO4. An RSPO2–4 chimera combining RSPO2 ZNRF3 binding with RSPO4 LGR4 binding was a "Superspondin" that exhibited enhanced ternary complex formation and 10-fold stronger signaling potency than RSPO2 and efficacy equivalent to RSPO2. An RSPO4–1 chimera combining RSPO4 ZNRF3 binding with RSPO1 LGR4 binding was a "Poorspondin" that exhibited signaling potency similar to RSPO1 and efficacy equivalent to RSPO4. Conferring increased ZNRF3 binding upon RSPO4 with amino acid substitutions L56F, I58L, and I63M enhanced its signaling potency and efficacy. Our results reveal the molecular basis for RSPOs1–4 activity differences and suggest that signaling potency is determined by ternary complex formation ability, whereas efficacy depends on ZNRF3 recruitment. High-potency RSPOs may be of value for regenerative medicine and/or therapeutic applications.

Introduction

R-spondins1–4 (RSPOs1–4) are secreted glycoproteins that potentiate Wnt signaling in vertebrates (de Lau et al., 2012; Jin and Yoon, 2012). RSPO actions are crucial for development (Aoki et al., 2007; Nam et al., 2007; Bell et al., 2008) and adult tissue homeostasis (Kim et al., 2005; Ootani et al., 2009; Sato et al., 2009), and aberrant RSPO signaling is implicated in cancer (Seshagiri et al., 2012). RSPOs are best characterized as growth factors for adult stem cells of the small intestine. Culture systems that permit in vitro growth of intestinal organoids from adult stem cells are dependent on exogenous RSPO1 (Sato et al., 2009, 2011; Sato and Clevers, 2013). RSPOs are thus valuable for regenerative medicine applications. RSPOs may also be of value as therapeutics. Exogenous RSPO1 administration alleviated colitis symptoms in a mouse model (Zhao et al., 2007) and provided protection against chemo- and radiation therapy–induced tissue damage in mice (Bhanja et al., 2009; Zhao et al., 2009; Takashima et al., 2011; Zhou et al., 2013).

RSPOs contain an N-terminal signal peptide followed by two cysteine-rich Furin-like domains, Fu1 and Fu2, a thrombospondin (TSP) domain, and a C-terminal basic region. The Fu1–Fu2 domain module is minimally sufficient to potentiate Wnt signaling (Kazanskaya et al., 2004). RSPOs signal through the leucine-rich repeat G protein–coupled receptors LGR4–6, and the transmembrane E3 ubiquitin ligases ZNRF3 and RNF43 (Carmon et al., 2011; de Lau et al., 2011, 2014; Glinka et al., 2011; Hao et al., 2012; Koo et al., 2012). LGR5 marks intestinal adult stem cells (Barker and Clevers, 2010). LGR4 is broadly expressed, but its coexpression with LGR5 in intestinal stem cells is crucial for their proliferation and crypt formation (de Lau et al., 2011). RSPOs do not appear to activate classic G protein–coupled receptor signaling pathways (Carmon et al., 2011); instead, RSPOs regulate Wnt receptor availability. ZNRF3/RNF43 ubiquitinylate Frizzled Wnt receptors to cause their internalization and degradation (Hao et al., 2012; Koo et al., 2012). RSPOs inhibit ZNRF3/RNF43 by forming a ternary complex with LGR4/5/6 and ZNRF3/RNF43, which leads to membrane clearance of the E3 ligase and thereby more Wnt receptors at the cell surface (Hao et al., 2012). LGR4/5/6 have a large extracellular domain (ECD) with 17 leucine-rich repeats (LRR) that provide the RSPO binding site, and ZNRF3/RNF43

This work was supported by a grant from the Oklahoma Center for Adult Stem Cell Research (A.A.P.) and in part by the National Institutes of Health National Institute of General Medical Sciences [Grant R01-GM104251] (A.A.P.).
The technology described in this manuscript is the subject of a patent application (A.A.P.).
dx.doi.org/10.1124/mol.114.095133.
[S] This article has supplemental material available at molpharm.aspetjournals.org.

ABBREVIATIONS: ANOVA, analysis of variance; BSA, bovine serum albumin; ECD, extracellular domain; Fu, Furin-like domain; LRR, leucine-rich repeat; MBP, maltose binding protein; RSPO, R-spondin; Th, thrombin protease cleavage site; TR-FRET, time-resolved fluorescence resonance energy transfer; TSP, thrombospondin.

have a small ECD for RSPO binding. Crystal structures of binary and ternary complexes (Chen et al., 2013; Peng et al., 2013a,b; Wang et al., 2013; Xu et al., 2013; Zebisch et al., 2013) and mutagenesis studies (Xie et al., 2013) indicated that distinct regions of RSPO Fu1–Fu2 contact the two receptors.

All four RSPOs signal by a common mechanism (Kim et al., 2008) and can promote the growth of intestinal stem cells (Kim et al., 2006), but significant functional differences exist. Genetic studies revealed roles for RSPO1, -2, -3, and -4 in sex determination, limb formation, placental development, and formation of toe- and fingernails, respectively (Blaydon et al., 2006; Parma et al., 2006; Aoki et al., 2007; Nam et al., 2007; Bell et al., 2008; Bruchle et al., 2008; Ishii et al., 2008). In cell-based Wnt signaling assays, RSPO2 and -3 were more active than RSPO1 and -4, and RSPO4 is considered the least active RSPO (Kim et al., 2008; Carmon et al., 2011; Zebisch et al., 2013). The RSPOs bind LGRs with nanomolar binding affinities (Carmon et al., 2011; de Lau et al., 2011; Glinka et al., 2011), but conflicting results were reported for the rank order of RSPOs1–4 binding to LGR4 (Carmon et al., 2011; Moad and Pioszak, 2013). RSPO2 and -3 bound ZNRF3 with nanomolar affinities, whereas RSPO1 and -4 had affinities in the micromolar range, with RSPO4 having the weakest ZNRF3 binding (Chen et al., 2013; Moad and Pioszak, 2013; Zebisch et al., 2013). We previously showed that RSPO2 and -3 were most competent for ternary complex formation and proposed that RSPO signaling potency is determined by ternary complex formation ability (Moad and Pioszak, 2013). Others have proposed that RSPO signaling potency is determined by ZNRF3/RNF43 binding ability (Zebisch et al., 2013). Here, we use purified wild-type, chimeric, and mutant RSPO Fu1–Fu2 proteins to examine the molecular basis for the differing signaling potencies and efficacies of RSPOs1–4. We show that RSPO4 has strong signaling potency despite its poor ZNRF3 binding, and importantly we generate novel chimeric and mutant RSPOs with signaling potencies greater than the natural RSPOs by engineering enhanced ternary complex formation ability.

Materials and Methods

Plasmids and Plasmid Construction. Bacterial expression plasmids for wild-type human RSPO2, -3, and -4 Fu1–Fu2 proteins as maltose binding protein (MBP)–thrombin protease cleavage site (Th)–RSPO Fu1–Fu2-H_6 fusions coexpressed with the bacterial disulfide bond isomerase DsbC were constructed with standard polymerase chain reaction and restriction endonuclease-based cloning techniques as described (Moad and Pioszak, 2013). The bacterial expression plasmids for wild-type MBP-Th-hRSPO1 Fu1–Fu2-H_6 and MBP-Th-hLGR4.23–383-H_6 were previously described (Moad and Pioszak, 2013). A bacterial expression plasmid for in vivo site-specific biotinylation of the human ZNRF3 ECD was constructed by swapping the BamHI-NotI ECD-encoding fragment from pAP353 (Moad and Pioszak, 2013) into a previously described plasmid (Pioszak et al., 2009) to enable coexpression of an MBP-Th-Avi tag-ZNRF3 ECD-H_6 fusion with the BirA biotin ligase. Chimeric RSPO and RSPO point mutant bacterial expression plasmids were constructed using either the Gibson Assembly cloning method with Gibson Assembly Master Mix (New England Biolabs, Ipswich, MA) or the QuikChange II site directed mutagenesis kit (Agilent Technologies, Wilmington, DE). A plasmid for expression of MBP-Th-hRSPO4 Fu1–Fu2-H_6 secreted from HEK293T cells was constructed by polymerase chain reaction amplifying the fusion protein-encoding fragment from the corresponding bacterial expression plasmid as an AgeI-KpnI fragment and ligating into plasmid pHLsec (Aricescu et al., 2006). Primer sequences are available from the authors upon request. The following plasmids were constructed for this work (amino acid residue numbers are indicated):

pAC018, pETDuet1/MBP-Th-RSPO2.22–144-H_6/DsbC; pAP355, pETDuet1/MBP-Th-RSPO3.22–146-H_6/DsbC; pAP356, pETDuet1/MBP-Th-RSPO4.21–138-H_6/DsbC; pMW012, pETDuet1/MBP-Th-RSPO4.21–138-H_6 (L56F, I58L, I63M)/DsbC; pMW015, pETDuet1/MBP-Th-RSPO2.22–76-RSPO4.72–138-H_6/DsbC [2–4 chimera]; pMW018, pETDuet1/MBP-Th-RSPO4.21–71-RSPO1.78–145-H_6/DsbC [4–1 chimera]; pMW017, pETDuet1/MBP-Th-Avi tag-ZNRF3.56–216-H_6/BirA; pTB025, pHLsec/MBP-Th-RSPO4.21–138-H_6; pTB032, pETDuet1/MBP-Th-RSPO2.22–144-H_6 (T111I)/DsbC.

Protein Expression and Purification. MBP-Th-RSPO Fu1–Fu2 and MBP-Th-LGR4 LRR1–14 proteins were expressed in *Escherichia coli* Origami B (DE3) cells as previously described (Hill and Pioszak, 2013; Moad and Pioszak, 2013). To facilitate in vivo biotinylation of MBP-Th-Avi tag-ZNRF3 ECD, Origami B (DE3) cells were cotransformed with plasmids pMW017 and pACYCDuet1/DsbC (Pioszak et al., 2009). Expression was carried out as for the other proteins except that the growth media included ampicillin and chloramphenicol and 50 μM biotin was added to the media upon induction with isopropyl-β-D-thiogalactopyranoside. The MBP-Th-RSPO Fu1–Fu2 and MBP-Th-LGR4 LRR1–14 fusion proteins were purified as previously described (Moad and Pioszak, 2013), except that 0.5–1 mM EDTA was included in the buffers for amylose, gel-filtration, and ion exchange chromatography and all buffers were degassed before use. The redox buffer conditions used for the RSPO2–4 chimera and RSPO4–1 chimera were 1 mM reduced glutathione/1 mM oxidized glutathione and 5 mM reduced glutathione/1 mM oxidized glutathione, respectively.

MBP-Th-biotin-ZNRF3 ECD-H_6 was purified as previously described for nonbiotinylated ZNRF3 ECD through the gel-filtration step (Moad and Pioszak, 2013). The peak gel-filtration fractions were pooled and digested with human α-thrombin protease at a 1:300 (thrombin weight:protein weight) ratio at 4°C overnight in gel filtration buffer. The digested sample was loaded onto a 5-ml monomeric avidin column (Thermo Scientific/Pierce, Rockford, IL) previously washed in 25 ml of binding buffer [50 mM Tris-HCl (pH 7.5), 10% (v/v) glycerol, 150 mM NaCl, and 0.5 mM EDTA]; 15 ml of elution buffer [50 mM Tris-HCl (pH 7.5), 5% (v/v) glycerol, 150 mM NaCl, and 2 mM biotin]; 25 ml of regeneration buffer (0.1 M glycine pH 2.8); and 25 ml of binding buffer. The column was washed with 200 ml of binding buffer and eluted with 25 ml of elution buffer. The eluted protein was concentrated using a 9 kDa molecular weight cutoff spin concentrator (Thermo Scientific/Pierce) and subjected to a final gel-filtration chromatography step as above.

RSPO Fu1–Fu2 proteins free of MBP were prepared by digesting their respective fusion proteins with human α-thrombin protease at a 1:300 ratio overnight at 4°C with dialysis to 50 mM Na/K phosphate (pH 7.0) and 5% (v/v) glycerol (S buffer A). The digested sample was applied to a 5 ml SP FF cation exchange column (GE Healthcare, Piscataway, NJ), washed in S buffer A, then eluted with a linear gradient of 0 to 1 M NaCl in S buffer A. Peak fractions were concentrated and subjected to a final gel-filtration step as above.

MBP-Th-RSPO4 Fu1–Fu2-H_6 was expressed as a secreted glycoprotein from HEK293T cells using polyethyleneimine-mediated transient transfection with plasmid pTB025 according to standard methods (Aricescu et al., 2006). The fusion protein was purified from the media on a 5 ml prepacked Ni-chelating sepharose column (GE Healthcare) followed by gel-filtration chromatography performed as for the other proteins.

All purified proteins were dialyzed to storage buffer containing 25 mM HEPES (pH 7.5), 50% (v/v) glycerol, and 150 mM NaCl for long-term storage at −80°C. Protein concentrations were determined by the Bradford method with a bovine serum albumin (BSA) standard curve and are stated in terms of the monomers. In some cases protein concentrations were verified by UV absorbance at 280 nm. Commercial recombinant RSPO1, -2, and -4 were from R&D Systems

(Minneapolis, MN), and they were reconstituted according to the manufacturer's directions.

Lanthascreen Time-Resolved Fluorescence Resonance Energy Transfer Assay for LGR4 ECD Binding. Labeling of proteins with donor and acceptor flourophores was performed as previously described (Moad and Pioszak, 2013) with the following alterations. MBP-Th-LGR4 was labeled with amine reactive Terbium chelate (Life Technologies, Grand Island, NY) in a volume of 125 μl with a 20-fold molar excess of label and incubation for 2 hours. MBP-Th-RSPO2 was labeled with Alexafluor488 5-TFPE (LifeTechnologies) in a volume of 2 ml with a fivefold molar excess of the label and incubation for 45 minutes. After quenching, the labeled proteins were separated from free label on a PD-10 gel filtration column (GE Healthcare). The equilibrium binding assays were performed as previously described in a buffer containing 50 mM HEPES (pH 7.5), 150 mM NaCl, 0.3% (v/v) Triton X-100, and 7 mg/ml fatty acid-free BSA (Moad and Pioszak, 2013). Binding data were analyzed with GraphPad Prism5.0 (GraphPad Software, San Diego, CA) as previously described (Moad and Pioszak, 2013).

AlphaLISA Luminescent Proximity Assay for ZNRF3 ECD Binding. Reaction conditions consisted of 50 mM 4-morpholinepropanesulfonic acid pH 7.4, 150 mM NaCl, 7 mg/ml fatty acid-free BSA, 15 or 20 μg/ml each streptavidin-coated donor and anti-MBP antibody-coated acceptor beads (PerkinElmer, Waltham, MA), 3 nM biotin-ZNRF3 ECD, and the indicated concentrations of MBP-Th-RSPO Fu1–Fu2 proteins. Reactions were prepared in the dark under green light and incubated for 3 hours at room temperature in the dark to reach equilibrium. Acceptor bead emission at 615 nm was measured in 384-well white optiplates (Greiner Bio-One, Monroe, NC) with a PolarStar Omega plate reader using filters for AlphaLISA (BMG Labtech, Ortenberg, Germany). Values were graphed with GraphPad Prism 5.0 (GraphPad Software). AlphaLISA saturation binding data were not fit by nonlinear regression because the two-bead format and consequent multivalent nature of the assay and the "hook effect" render standard binding equations inappropriate for this assay.

AlphaLISA Luminescent Proximity Assay for Ternary Complex Formation. Buffer conditions were the same as for the AlphaLISA ZNRF3 binding assay and the reactions contained 5 nM biotin-ZNRF3 ECD, 5 nM MBP-Th-LGR4 ECD, and the indicated concentrations of MBP-free RSPO Fu1–Fu2 proteins. The reactions were incubated 4 hours to reach equilibrium before reading emission at 615 nm as above.

TOPFLASH Wnt/β-catenin Signaling Reporter Assay. This assay was performed essentially as described (Moad and Pioszak, 2013). HEK293T cells seeded in 96-well cell culture plates in DMEM + 10% fetal bovine serum + 50 units/ml penicillin, 50 μg/ml streptomycin were transiently transfected with a plasmid mixture containing 50 ng of Super8x TOPFLASH reporter, 10 ng pRL-TK, and 40 ng empty pcDNA3.1 (per well) using FuGENE HD (Promega, Madison, WI). The recombinant RSPO proteins were dialyzed to PBS, pH 7.4 overnight at 4°C, their concentrations were determined by Bradford assay, and they were diluted as indicated in 1:6 diluted Wnt3a conditioned media. The transfected cells were treated with the proteins for 24 hours. Firefly and *Renilla* luciferase activities were measured with a Dual Luciferase Reporter assay kit (Promega). Signaling response was plotted as the Firefly/*Renilla* ratio with normalization to controls as indicated. GraphPad Prism 5.0 (GraphPad Software) was used for nonlinear regression fitting of the dose-response curves to a three-parameter, fixed slope log (agonist) versus response equation.

Statistical Analysis. Results are presented as the mean ± standard error of the mean and significance was determined by unpaired t test or one-way analysis of variance (ANOVA) followed by Tukey's multiple comparison post hoc test, as appropriate, using GraphPad Prism 5.0 (GraphPad Software). In tables and figures, P values are represented as $^{*}P < 0.05$, $^{**}P < 0.01$, and $^{***}P < 0.001$.

Amino Acid Sequence Alignments, Structure Analysis, and Figure Preparation. Amino acid sequence alignments were performed with ClustalW2 and sequence alignment figures were generated with ESpript3.0 (Goujon et al., 2010; Robert and Gouet, 2014). Crystal structure analyses and structure figure preparation used PyMol (Schrödinger, New York).

Results

Improved Bacterial Production of Recombinant R-spondins and Re-examination of RSPOs1–4 Signaling and Receptor Binding Activities. We previously reported novel methodology for bacterial production of recombinant RSPOs produced as MBP-RSPO Fu1-Fu2-H_6 fusion proteins (Moad and Pioszak, 2013). To facilitate additional studies we bacterially expressed and purified the four human RSPO Fu1–Fu2 proteins as MBP- Th-RSPO Fu1–Fu2-H_6 fusion proteins to allow removal of MBP by thrombin digest if necessary. In the course of our studies we discovered changes to the purification protocol that yielded a marked improvement in the behavior of the RSPO proteins on gel-filtration chromatography compared with our previous results. Degassing the purification buffers and inclusion of 0.5–1 mM EDTA in the buffers allowed us to obtain sharp symmetric "folded" peaks on gel-filtration (Fig. 1A) as opposed to the broad asymmetric peaks previously obtained (Moad and Pioszak, 2013). The four resulting MBP-Th-RSPO Fu1–Fu2-H_6 proteins were highly purified (Fig. 1B).

In light of the improved purifications of the wild-type MBP-Th-RSPO Fu1–Fu2-H_6 fusion proteins we re-examined their ability to potentiate low-dose Wnt3a activation of the canonical

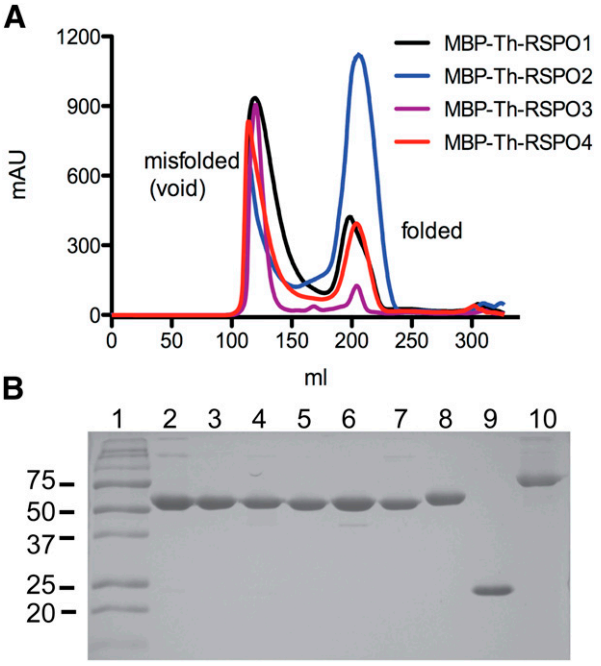

Fig. 1. Recombinant protein production. (A) Superdex200 HR gel-filtration chromatograms for the four wild-type MBP-Th-RSPO Fu1–Fu2-H_6 proteins produced in *E. coli*. (B) Nonreducing SDS-PAGE showing selected purified proteins used in this study. 2.5 μg of each protein was loaded per lane and the gel was stained with Coomassie brilliant blue. Molecular mass markers are shown in kilodaltons. Lanes are as follows: 1, marker; 2, MBP-Th-RSPO1 Fu1–Fu2; 3, MBP-Th-RSPO2 Fu1–Fu2; 4, MBP-Th-RSPO3 Fu1–Fu2; 5, MBP-Th-RSPO4 Fu1–Fu2; 6, MBP-Th-RSPO2–4 Fu1–Fu2; 7, MBP-Th-RSPO4–1 Fu1–Fu2; 8, glycosylated MBP-Th-RSPO4 Fu1–Fu2 produced in HEK293T cells; 9, biotin-ZNRF3 ECD; 10, MBP-Th-LGR4 LRR1–14. All recombinant proteins other than N-glycosylated MBP-Th-RSPO4 Fu1–Fu2 were produced in *E. coli*.

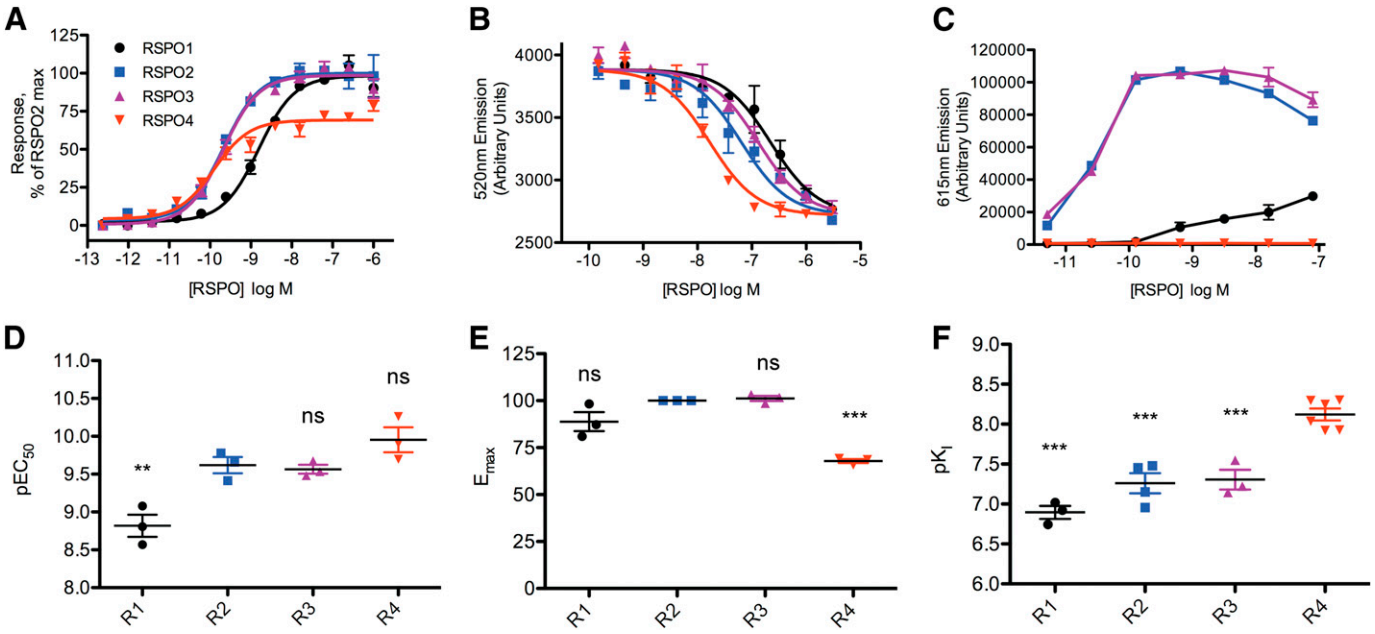

Fig. 2. Signaling and receptor binding activities of bacterially produced recombinant MBP-Th-RSPOs1–4 Fu1-Fu2 proteins. (A) Potentiation of Wnt3a activation of the canonical Wnt/β-catenin pathway. HEK293T cells transfected with TOPFLASH firefly luciferase reporter and *Renilla* luciferase control plasmids were treated with the indicated concentrations of MBP-Th-RSPO Fu1–Fu2 proteins in 1:6 diluted Wnt3a conditioned media. (B) Binding of MBP-Th-RSPOs1–4 Fu1–Fu2 proteins to the LGR4 ECD in vitro by TR-FRET competition assay. Tb-chelate–labeled MBP-Th-LGR4 LRR1–14 (20 nM) and AF488-labeled MBP-Th-RSPO2 Fu1–Fu2 (125 nM) were incubated with the indicated concentrations of unlabeled MBP-Th-RSPO Fu1–Fu2 proteins. (C) AlphaLISA luminescent proximity assay for ZNRF3 ECD binding. The indicated concentrations of MBP-Th-RSPO Fu1–Fu2 proteins were incubated with 3 nM biotin-ZNRF3 ECD. Donor and acceptor beads were at 20 μg/ml each. Data shown for (A–C) are representative of at least three independent experiments each performed in duplicate. The error bars represent the S.E.M. of the experiment. (D, E, and F) Vertical scatter plots showing the pEC_{50}, E_{max}, and pK_I values obtained from replicate independent signaling and LGR4 binding experiments as in (A and B). The mean values and error bars representing the S.E.M. of the replicates are denoted. Statistical significance ($^{**}P < 0.01$ and $^{***}P < 0.001$) from one-way ANOVA with Tukey's test is shown for comparison with RSPO2 in (D and E) and for comparison with RSPO4 in (F). ns, not significant.

Wnt/β-catenin pathway in a TOPFLASH dual luciferase reporter signaling assay. The HEK293T cells used for this assay express LGR4, ZNRF3, and Wnt receptors. RSPO2 and -3 exhibited identical strong potencies and maximal responses, RSPO1 exhibited ~6-fold reduced potency compared with RSPO2/3 while retaining a similar maximal response, and RSPO4 exhibited a potency slightly stronger than RSPO2/3 but a lower maximal response equivalent to ~70% of that observed for RSPO2/3 (Fig. 2, A, D, and E; Table 1). In this set of experiments comparing the four wild types to each other, the RSPO4 potency was not statistically significantly different from RSPO2 (Table 1), but in other experiments comparing RSPO2 and -4 to mutant proteins the RSPO2 versus RSPO4 potency difference did reach statistical significance (Table 4). Conservatively speaking, the rank order of potencies was thus RSPO2/3/4 > RSPO1 and the rank order of the maximal responses was RSPO1/2/3 > RSPO4. These results were consistent with our previous results (Moad and Pioszak, 2013), with the exceptions that each of the newly purified RSPOs was a bit more potent and we previously observed a potency rank order of RSPO2/3 > RSPO4 > RSPO1. Presumably the differences observed here resulted from the improved purification protocol.

The LGR4 ECD binding abilities of the newly purified MBP-Th-RSPO Fu1–Fu2-H_6 proteins were examined in an in vitro LanthaScreen time-resolved fluorescence resonance energy transfer (TR-FRET) competition–binding assay. RSPO4 bound the LGR4 ECD with an affinity ~7-fold stronger than those of RSPO2 and -3, which were equivalent (Fig. 2, B and F; Table 2). RSPO1 affinity for LGR4 was slightly diminished compared with RSPO2/3 (Fig. 2, B and F), although this did not reach statistical significance by one-way ANOVA and Tukey's test comparing RSPO1 versus RSPO2 or -3. These LGR4 binding data are in agreement with our previous findings (Moad and Pioszak, 2013). We were unsuccessful in applying the TR-FRET assay to ZNRF3 binding (data not shown), so an AlphaLISA luminescent proximity assay was developed to measure ZNRF3 ECD binding. In this assay, biotinylated ZNRF3 ECD is attached to the surface of streptavidin-coated donor beads, and the MBP-Th-RSPO fusion proteins are attached to the surface of α-MBP–coated acceptor beads. Receptor-ligand interaction is detected by measuring 615 nm emission from the acceptor beads, which is dependent on singlet oxygen molecules released from nearby donor beads. Site-specific in vivo biotinylation of the ZNRF3 ECD was carried out by bacterial coexpression of N-terminally Avi-tagged ZNRF3 ECD with the biotin ligase BirA. Biotin-ZNRF3 ECD was purified to homogeneity (Fig. 1B). In a saturation binding assay format, RSPO2 and -3 exhibited similar strong binding affinities for ZNRF3, RSPO1 had much

TABLE 1

Summary of signaling data for wild-type RSPOs1–4 Fu1–Fu2

E_{max} values are % of MBP-Th-RSPO2. The number of observations is indicated in parentheses.

R-spondin	pEC_{50} ± S.E.M.	E_{max} ± S.E.M.
MBP-Th-RSPO1	8.82 ± 0.15** (3)	88.82 ± 5.05 (3)
MBP-Th-RSPO2	9.62 ± 0.11 (3)	100 (3)
MBP-Th-RSPO3	9.56 ± 0.06 (3)	101.2 ± 1.39 (3)
MBP-Th-RSPO4	9.95 ± 0.16 (3)	67.85 ± 1.07*** (3)

$^{**}P < 0.01$; $^{***}P < 0.001$ versus MBP-Th-RSPO2 by one-way ANOVA with Tukey's multiple comparison test.

TABLE 2
Summary of LGR4 ECD binding data for wild-type, chimeric, and mutant R-spondins
The number of observations is indicated in parentheses.

R-spondin	pK_I ± S.E.M.
MBP-Th-RSPO1	6.90 ± 0.08*** (3)
MBP-Th-RSPO2	7.26 ± 0.13*** (4)
MBP-Th-RSPO3	7.31 ± 0.12*** (3)
MBP-Th-RSPO4	8.12 ± 0.07 (6)
MBP-Th-RSPO2-4	8.36 ± 0.04 (3)
MBP-Th-RSPO4-1	7.32 ± 0.11*** (4)
MBP-Th-RSPO2 T111I	7.57 ± 0.12 (3)

***$P < 0.001$ versus MBP-Th-RSPO4 by one-way ANOVA with Tukey's multiple comparison test, except for RSPO2 T111I, which was compared with RSPO2.

weaker affinity, and RSPO4 binding was not detected (Fig. 2C), in agreement with our previous findings using a native gel mobility shift assay (Moad and Pioszak, 2013) and with those of Zebisch et al. (2013) using surface plasmon resonance.

Our signaling and receptor binding results with bacterially produced wild-type RSPOs are in good agreement with those of other groups using RSPOs produced in eukaryotic systems with the notable exceptions of the strong signaling potency and strong LGR4 binding affinity of our RSPO4. Other groups reported RSPO4 to have the weakest signaling potency and weakest LGR4 affinity (Kim et al., 2008; Carmon et al., 2011; Zebisch et al., 2013). In our hands, the signaling potency rank order of commercial recombinant RSPO1, -2, and -4 proteins (R&D Systems) was RSPO2 > RSPO1 > RSPO4 consistent with the findings of other groups (Supplemental Fig. 1). The commercial RSPO1 and -4 proteins are full-length, whereas RSPO2 is the Fu1–Fu2-TSP fragment. Seeking the source of the RSPO4 discrepancy, we expressed and purified glycosylated MBP-Th-RSPO4 Fu1–Fu2-H_6 secreted from HEK293T cells (Fig. 1B) and compared its signaling activity to that of the equivalent bacterially produced protein. The HEK293T cell-produced protein exhibited signaling potency and efficacy similar to the bacterially produced protein (Fig. 3A; Table 3). A sensitive t test indicated that the pEC_{50} values were statistically significantly different, but the effect was not dramatic and did not appear to be sufficient to account for the discrepancy. Comparing the signaling activities of bacterially produced MBP-Th-RSPO4 Fu1–Fu2, MBP-free RSPO4 Fu1–Fu2 (generated by thrombin cleavage of the bacterially produced protein and purification of the Fu1–Fu2 fragment), and R&D Systems full-length RSPO4 indicated that MBP did not alter signaling potency and that the minimal Fu1–Fu2 domain module proteins were more potent than the full-length protein (Fig. 3B). Notably, the commercial full-length RSPO4 exhibited LGR4 ECD binding affinity identical to bacterially produced MBP-Th-RSPO4 Fu1–Fu2 (Fig. 3C; Table 3). These data suggest that the RSPO4 TSP domain and/or C-terminal basic region may have an inhibitory effect on RSPO4 signaling activity, which may explain the discrepancy.

Engineering a Highly Potent and Efficacious Chimeric "Superspondin.". The RSPOs1–4 Fu1–Fu2 signaling and receptor binding results presented thus far are consistent with our previous proposal that RSPO signaling potency is determined by its ability to form the ternary complex (Moad and Pioszak, 2013), and we further hypothesize that RSPO signaling efficacy is largely determined by ZNRF3 recruitment into the complex. This hypothesis predicts that it should be possible to construct a "Superspondin" with enhanced signaling potency by combining the strong ZNRF3 binding of RSPO2 with the strong LGR4 binding of RSPO4. To this end, we constructed and purified a chimeric MBP-Th-RSPO2–4 Fu1–Fu2 molecule. Chimera design was aided by consulting the crystal structure of the ternary RSPO1 Fu1–Fu2:LGR5 ECD:RNF43 ECD complex (Chen et al., 2013) (Fig. 4A) and an amino acid sequence alignment of the four RSPOs (Supplemental Fig. 2). Our design resulted in a chimeric RSPO2–4 Fu1–Fu2 molecule with a junction point between the second and third β-hairpin structural elements of Fu1 such that the ZNRF3 interacting region of RSPO2 was fused to the LGR4 interacting region of RSPO4 (Fig. 4B). The bacterially produced recombinant MBP-Th-RSPO2–4 Fu1–Fu2 chimera exhibited 10-fold stronger signaling potency than RSPO2 and efficacy equivalent to RSPO2 (Fig. 5, A, D, and E; Table 4). The RSPO2–4 chimera bound the ZNRF3 (Fig. 5B) and LGR4 (Fig. 5, C and F; Table 2) ECDs with affinities similar to RSPO2 and RSPO4, respectively.

An AlphaLISA assay was developed to allow direct assessment of ternary complex formation. This assay was similar

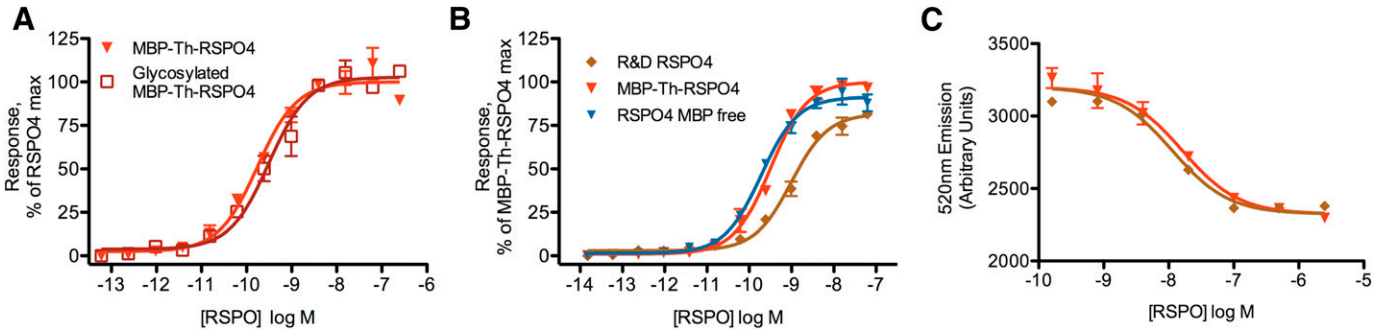

Fig. 3. Signaling and LGR4 binding activities of recombinant RSPO4 Fu1–Fu2 proteins produced in bacteria or HEK293T cells and commercial full-length RSPO4 produced in CHO cells. (A) Signaling assay for MBP-Th-RSPO4 Fu1–Fu2 proteins produced in bacteria or HEK293T cells (glycosylated). Data shown are representative of three independent experiments each performed in duplicate and the error bars represent the S.E.M. of the experiment. (B) Signaling assay for bacterially produced MBP-Th-RSPO4 Fu1–Fu2 and MBP-free RSPO4 Fu1–Fu2 compared with commercial full-length RSPO4 produced in CHO cells (R&D Systems). Data shown are representative of two independent experiments each performed in duplicate and the error bars represent the S.E.M. of the experiment. (C) TR-FRET LGR4 ECD competition–binding assay as in Fig. 2B comparing bacterially produced MBP-Th-RSPO4 Fu1–Fu2 and commercial full-length RSPO4 (R&D Systems). Data shown are representative of three independent experiments each performed in duplicate, and the error bars represent the S.E.M. of the experiment.

TABLE 3
Summary of signaling and LGR4 ECD binding data for RSPO4 proteins produced in different expression systems
E_{max} values are % of bacterially produced MBP-Th-RSPO4. The number of observations is indicated in parentheses.

R-spondin (expression system)	pEC_{50} ± S.E.M.	E_{max} ± S.E.M.	pK_I ± S.E.M.
MBP-Th-RSPO4[a] (*E. coli*)	9.80 ± 0.04 (3)	100 (3)	8.28 ± 0.14 (3)
MBP-Th-RSPO4[a] (HEK293T)	9.48 ± 0.04** (3)	94.77 ± 4.63 (3)	—
R&D RSPO4[b] (CHO)	—	—	8.23 ± 0.11 (3)

[a]Fu1-Fu2 domain module.
[b]Full-length protein.
**$P < 0.01$ versus bacterially produced MBP-Th-RSPO4 by unpaired t test.

to the ZNRF3 ECD binding assay, except that MBP-Th-LGR4 ECD was attached to the surface of the α-MBP–coated acceptor beads, and MBP-free RSPO Fu1–Fu2 proteins were used to bring the receptor-coated beads into proximity. MBP-free RSPO2–4 chimera and RSPO2 were generated by thrombin digestion of their respective fusion proteins followed by purification to isolate the RSPO Fu1–Fu2. A gel-filtration chromatography step was included in the purifications to eliminate the possibility of contaminating undigested MBP-Th-RSPO fusion protein. In a saturation binding assay format, the RSPO2–4 chimera exhibited enhanced ability to bring the two receptors together compared with RSPO2 (Fig. 6). Control experiments indicated that the two receptors did not associate in the absence of RSPOs and signal generation was dependent on the presence of both receptors (Supplemental Fig. 3). These results suggested that the enhanced signaling potency of the RSPO2–4 chimera resulted from its increased ability to form the ternary complex.

Engineering a Low-Potency, Low-Efficacy Chimeric "Poorspondin.". It follows that if the RSPO2–4 chimera is a Superspondin, then a chimeric RSPO4-1 molecule combining the poor ZNRF3 binding of RSPO4 with the weak LGR4 binding of RSPO1 should be a "Poorspondin" with weak signaling potency and efficacy. To test this hypothesis, we constructed and purified an MBP-Th-RSPO4–1 Fu1–Fu2 chimera. The chimera junction point was the same as for the Superspondin (Fig. 4B). The bacterially produced recombinant MBP-Th-RSPO4–1 Fu1–Fu2 chimera exhibited potency in the signaling assay similar to RSPO1 and efficacy equivalent to that of RSPO4 (Fig. 7, A, C, and D; Table 5). The RSPO4–1 chimera bound the LGR4 ECD with significantly weaker affinity than RSPO4, but unexpectedly it retained slightly better binding affinity for LGR4 than RSPO1 (Fig. 7, B and E; Table 2). The difference in mean pK_I values for RSPO1 versus the RSPO4–1 chimera was statistically significant ($P < 0.05$) as assessed by one-way ANOVA with Tukey's post hoc test.

Enhancing Signaling Potency by Introducing Amino Acid Substitutions into RSPO4 or RSPO2. We sought to generate a high-potency RSPO by determining the amino acid substitutions required to confer upon RSPO4 the strong ZNRF3 binding of RSPO2. To understand the structural basis for the high-affinity ZNRF3 binding of RSPO2 and rationalize why RSPO4 has such weak ZNRF3 binding affinity, we consulted the crystal structures of the binary RSPO1 and -2 Fu1–Fu2:ZNRF3 ECD complexes (Peng et al., 2013b; Zebisch et al., 2013) (Fig. 8A) and an amino acid sequence alignment of the four human RSPOs for the ZNRF3/RNF43-interacting region, which is comprised of the first two β-hairpin structural elements of Fu1 (Fig. 8B). The structures and mutagenesis data (Peng et al., 2013b; Xie et al., 2013; Zebisch et al., 2013) indicated that two conserved RSPO residues are most critical for ZNRF3/RNF43 binding: R66 and Q71 (RSPO1 numbering), which are located on the β-strands of the second β-hairpin of Fu1 and face into a shallow cleft on the ZNRF3/RNF43 surface (Figs. 4B and 8A). RSPOs1–4 have a variable residue at position 69 (RSPO1 numbering) on the tip of the loop of the second β-hairpin of Fu1 (Fig. 8B). This residue, either an isoleucine or a methionine, fits into a hydrophobic pocket of ZNRF3 formed by residues I98, V195, and A201. Methionine at this position was previously shown to contribute to the increased ZNRF3 binding affinity of RSPO2 (Zebisch et al., 2013) but not enough to account for the dramatic difference in ZNRF3/RNF43 binding affinities of RSPO2/3 compared with RSPO1/4. Two additional residues in RSPO β-strand 3 at positions 62 and 64 (RSPO1 numbering) provide contacts to ZNRF3 and differ among the four RSPOs (Fig. 8B). We reasoned that RSPO4 residues L56 and I58 provide less favorable contacts with ZNRF3 L104 and H102 than RSPO2 F61 and L63. Indeed, the recombinant MBP-Th-RSPO4 Fu1–Fu2-H_6 [L56F/I58L/I63M] triple mutant

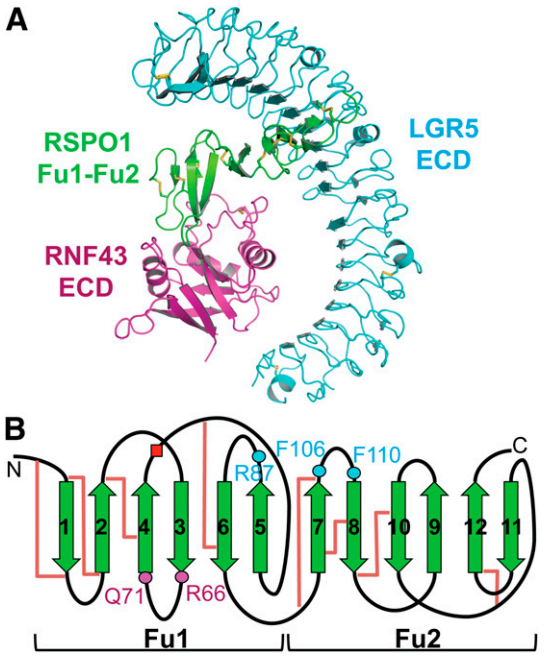

Fig. 4. Architecture of the ternary complex and chimera design. (A) Crystal structure of the ternary RSPO1 Fu1–Fu2:LGR5 ECD:RNF43 ECD complex (PDB ID 4KNG). (B) Topology of the RSPO Fu1–Fu2 module highlighting ZNRF3/RNF43 and LGR4/5/6 interacting regions and chimera fusion point. Disulfide bonds are shown as brown connecting lines, cyan circles show conserved RSPO residues critical for interaction with LGR4/5/6, magenta circles highlight conserved RSPO residues critical for interaction with ZNRF3/RNF43, and the red square indicates the chimera junction point. Residue numbers correspond to RSPO1.

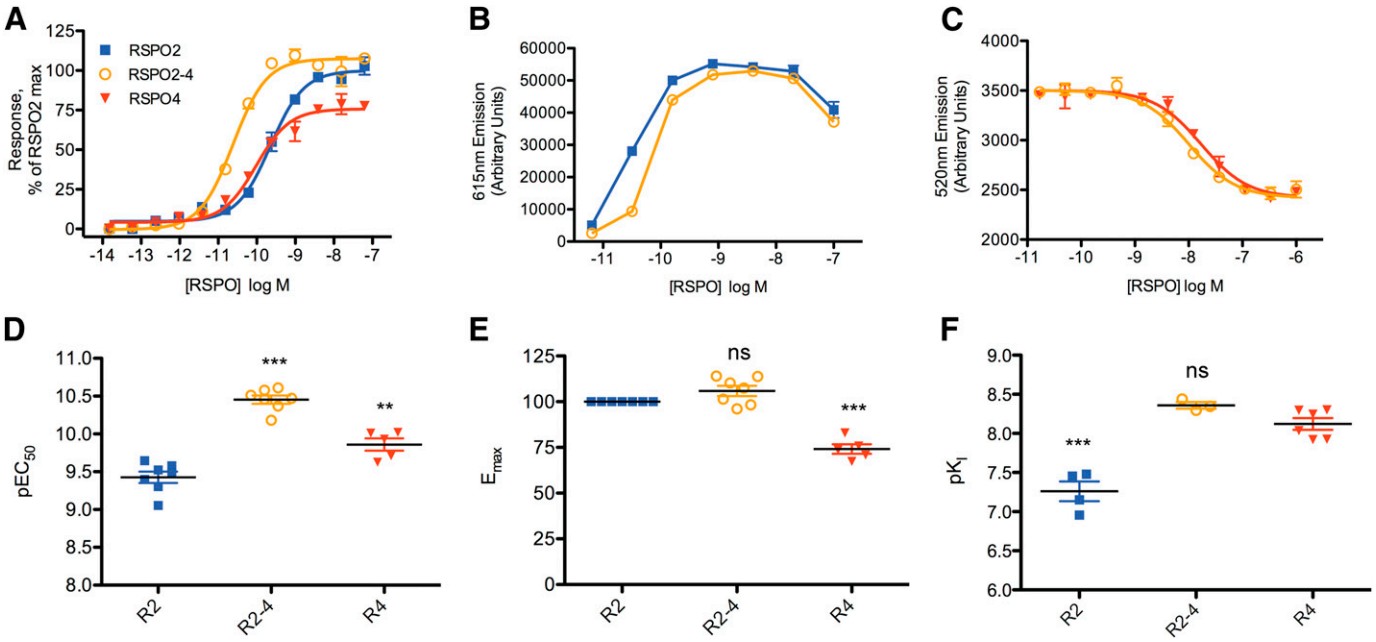

Fig. 5. Signaling and receptor binding activities of the chimeric RSPO2–4 "Superspondin." (A) TOPFLASH Wnt signaling assay with the indicated MBP-Th-RSPO Fu1–Fu2 proteins. Data shown are representative of at least five experiments each performed in duplicate. The error bars represent the S.E.M. of the experiment. (B) ZNRF3 binding AlphaLISA assay as in Fig. 2C except that donor and acceptor beads were at 15 μg/ml each. Data shown are representative of three independent experiments each performed in duplicate. The error bars represent the S.E.M. of the experiment. (C) LGR4 binding TR-FRET competition assay as in Fig. 2B. Data shown are representative of at least three independent experiments each performed in duplicate and the error bars represent S.E.M. of the experiment. (D, E, and F) Vertical scatter plots showing the pEC_{50}, E_{max}, and pK_I values obtained from replicate independent signaling and LGR4 binding experiments as in (A and C). The mean values and error bars representing the S.E.M. of the replicates are denoted. Statistical significance ($^{**}P < 0.01$ and $^{***}P < 0.001$) from one-way ANOVA with Tukey's test is shown for comparison with RSPO2 in (D and E) and for comparison with RSPO4 in (F). ns, not significant.

exhibited enhanced ZNRF3 binding (Fig. 8C), albeit not as strong as RSPO2 or the 2–4 chimera, and signaling potency ~6-fold stronger than RSPO2 and efficacy equivalent to RSPO2 (Fig. 8D; Table 4).

We next sought to identify amino acid substitutions in RSPO2 that would confer upon it the strong LGR4 binding of RSPO4 and thereby enhance its signaling potency, but this approach turned out to be more difficult. The crystal structure of the binary RSPO1 Fu1–Fu2:LGR4 ECD complex (Wang et al., 2013) (Supplemental Fig. 4A) and mutagenesis data (Xie et al., 2013) indicated that three conserved RSPO residues are most critical for LGR binding: R87 (RSPO1 numbering), which is located at the end of β-strand 5 in Fu1, and F106 and F110, which are situated on the loop of the first β-hairpin of Fu2 (Fig. 4B and Supplemental Fig. 4B). R87 forms salt-bridge and/or hydrogen bonds with a cluster of aspartate residues in LGR4 (D137, 161, and 162), whereas F106 and F110 form hydrophobic interactions with W159, A181, V204, and V205 of LGR4. RSPO1 T112, which is adjacent to F106 and F110, is conserved in RSPOs1–3, but this position is an isoleucine in RSPO4. We reasoned that an isoleucine at this position might provide additional hydrophobic/van der Waals contacts to LGR4 W159 and/or H157 to increase binding affinity (Supplemental Fig. 4A). The recombinant MBP-Th-RSPO2 Fu1–Fu2-H_6 [T111I] mutant exhibited LGR4 binding affinity that was not statistically significantly different from that of RSPO2 (Table 2), but the trend was toward improved LGR4 affinity (Supplemental Fig. 4, C and E). The RSPO2 [T111I] mutant exhibited slightly stronger signaling potency than RSPO2 and this result did reach statistical significance (Table 4), but it was not a dramatic effect (Supplemental Fig. 4, D, F, and G). We also constructed and tested the RSPO2 S77D single and S77D/P88Q/K107Q triple mutant proteins, which were chosen as candidates for increased LGR4 affinity based on sequence alignment and structural considerations, but these mutants did not exhibit enhanced signaling potencies (data not shown).

Discussion

R-spondins have critical functions in adult tissue homeostasis via their actions on adult stem cells. RSPOs are of considerable value for regenerative medicine applications and they may also be of value as therapeutic molecules. Here, we used purified wild-type, chimeric, and mutant RSPO Fu1–Fu2 proteins to analyze the molecular basis for the differing

TABLE 4
Summary of signaling data for RSPO superspondin and mutants
E_{max} values are % of MBP-Th-RSPO2. The number of observations is indicated in parentheses.

R-spondin	pEC_{50} ± S.E.M.	E_{max} ± S.E.M.
MBP-Th-RSPO2	9.43 ± 0.08 (7)	100 (7)
MBP-Th-RSPO4	9.86 ± 0.08** (5)	74.14 ± 2.62*** (5)
MBP-Th-RSPO2-4	10.45 ± 0.05*** (7)	105.9 ± 2.78 (7)
MBP-Th-RSPO4-triple	10.19 ± 0.16*** (4)	97.94 ± 7.51 (4)
MBP-Th-RSPO2[a]	9.37 ± 0.08 (3)	100 (3)
MBP-Th-RSPO4[a]	9.69 ± 0.04* (3)	74.25 ± 2.26*** (3)
MBP-Th-RSPO2 T111I[a]	9.75 ± 0.07* (3)	103.1 ± 2.40 (3)

[a]RSPO2 T111I was compared with RSPO2 and -4 in a separate set of experiments so the controls are listed twice.
$^{*}P < 0.05$; $^{**}P < 0.01$; $^{***}P < 0.001$ versus MBP-Th-RSPO2 by one-way ANOVA with Tukey's multiple comparison test.

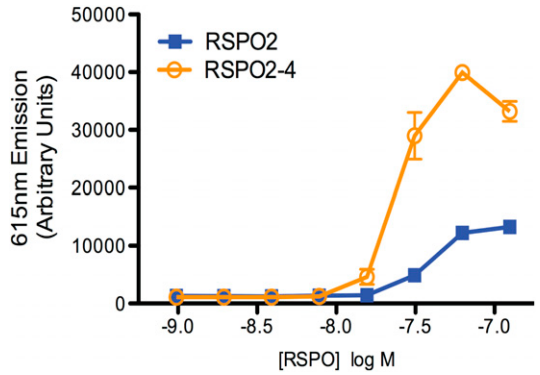

Fig. 6. AlphaLISA assay for ternary complex formation. The indicated concentrations of bacterially produced MBP-free RSPO2 and 2–4 chimera Fu1–Fu2 proteins were incubated with 5 nM biotin-ZNRF3 ECD, 5 nM MBP-Th-LGR4 LRR1–14 and 15 μg/ml each donor and acceptor beads. Data shown are representative of two independent experiments each performed in duplicate. The error bars represent the S.E.M. of the experiment.

signaling potencies and efficacies of the four human RSPOs, and importantly we generated novel RSPO molecules that exhibit significantly stronger signaling potencies than the natural RSPOs. We previously reported bacterial production of functional RSPOs1–4 Fu1–Fu2 proteins using our unique hybrid methodology combining disulfide bond formation in vivo during expression with in vitro "disulfide shuffling." We further improved upon this methodology with the findings that degassing the purification buffers and including EDTA in the buffers yielded significantly improved behavior of the RSPO proteins on gel-filtration chromatography (Fig. 1). The degassing and presence of EDTA may provide a more stable environment for the cysteine redox chemistry during in vitro disulfide shuffling. The newly purified proteins were a bit more active in the signaling assay than our previously used proteins (Moad and Pioszak, 2013), and they appeared to be equally active to those produced in eukaryotic expression systems as demonstrated for RSPO4 (Fig. 3A).

Our signaling results for the wild-type RSPOs agree with previous reports with the exception of the strong signaling potency we observed for RSPO4 (Fig. 2, A, D, and E). The presence of MBP in the fusion protein and the lack of glycosylation of the bacterially produced protein were ruled out as causes of the discrepancy (Fig. 3, A and B). In our hands the minimal RSPO4 Fu1–Fu2 fragment was more active than commercial full-length RSPO4, although they exhibited equal LGR4 binding affinities (Fig. 3, B and C). These data suggest that the RSPO4 TSP domain and/or C-terminal basic region may inhibit its signaling activity. In contrast, the TSP domain of RSPO1 enhanced its signaling activity (Kim et al., 2008). Moreover, the RSPO2 and -3 TSP domains bind syndecan 4 (Glinka et al., 2011; Ohkawara et al., 2011), which may increase the RSPO concentration at the cell surface to enhance their signaling activities. Consistent with these studies, we observed that the commercial RSPO1 and -2 proteins (with TSP domains) were more potent in the signaling

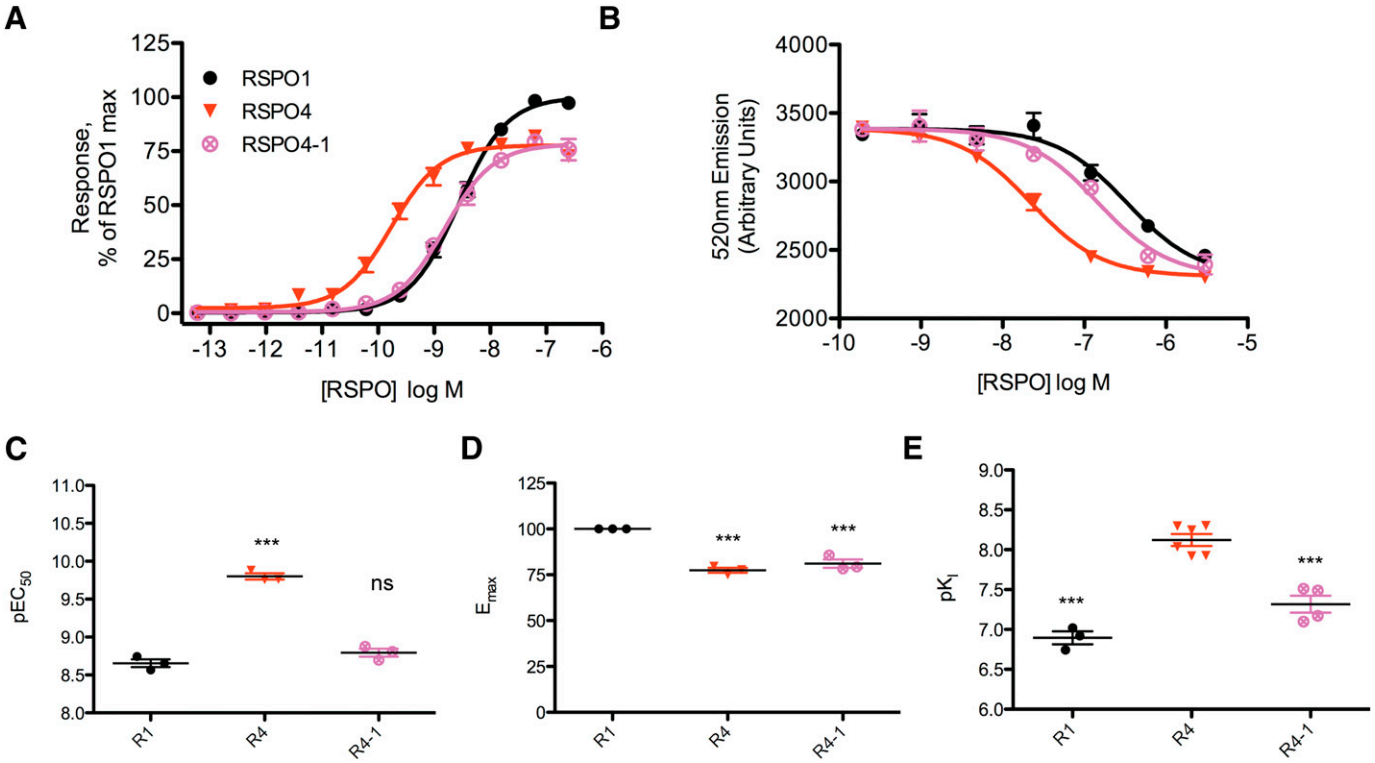

Fig. 7. Signaling and LGR4 binding activities of the chimeric RSPO4-1 "Poorspondin." (A) TOPFLASH Wnt signaling assay with the indicated MBP-Th-RSPO Fu1–Fu2 proteins. Data shown are representative of three independent experiments each performed in duplicate. The error bars represent the S.E.M. of the experiment. (B) LGR4 binding TR-FRET competition assay as in Fig. 2B. Data shown are representative of at least three independent experiments each performed in duplicate. The error bars represent the S.E.M. of the experiment. (C, D, and E) Vertical scatter plots showing the pEC_{50}, E_{max}, and pK_I values obtained from replicate independent signaling and LGR4 binding experiments as in (A and B). The mean values and error bars representing the S.E.M. of the replicates are denoted. Statistical significance (***$P < 0.001$) from one-way ANOVA with Tukey's test is shown for comparison with RSPO1 in (C and D) and for comparison with RSPO4 in (E).

TABLE 5
Summary of signaling data for RSPO poorspondin
E_{max} values are % of MBP-Th-RSPO1. The number of observations is indicated in parentheses.

R-spondin	pEC_{50} ± S.E.M.	E_{max} ± S.E.M.
MBP-Th-RSPO1	8.66 ± 0.05 (3)	100 (3)
MBP-Th-RSPO4	9.80 ± 0.04*** (3)	77.45 ± 1.36*** (3)
MBP-Th-RSPO4-1	8.79 ± 0.05 (3)	81.06 ± 2.31*** (3)

***$P < 0.001$ versus MBP-Th-RSPO1 by one-way ANOVA with Tukey's multiple comparison test.

assay than the minimal RSPO1 and -2 Fu1–Fu2 proteins (compare Fig. 2 and Supplemental Fig. 1). RSPO4 thus appears unique with respect to the possible negative effect of its TSP domain. Resolving the roles of the RSPO TSP domains in regulating their activities is an area for future study. Our results remain at odds with previous reports that the minimal RSPO4 Fu1–Fu2 fragment was relatively inactive (Kim et al., 2008; Zebisch et al., 2013), but in these studies the authors used a transfection assay with RSPO-encoding plasmids so methodological differences could contribute to the discrepancy.

Our LGR4 ECD binding assay results for the wild-type RSPOs agreed with our previous findings using the TR-FRET assay and a native gel mobility shift assay (Moad and Pioszak, 2013) that the rank order of affinities is RSPO4 > RSPO2/3 > RSPO1. However, Carmon et al. (2011) reported that RSPO4 had the weakest binding affinity for full-length LGR4 in a whole-cell binding assay. The basis for this discrepancy is unclear, but differences in binding assay methodology may have contributed. We cannot formally rule out the possibility that the lack of glycosylation of the LGR4 ECD used in the TR-FRET assay is responsible for the discrepancy, but it seems unlikely because our binding and signaling assay results are entirely consistent and the LGR4 in the HEK293T cells used for the signaling assay would be glycosylated. In contrast to the RSPO4 signaling potency and LGR4 binding discrepancies, our ZNRF3 ECD binding AlphaLISA assay results are in complete agreement with a previous report that the rank order of affinities is RSPO2/3 > > RSPO1 > RSPO4 (Zebisch et al., 2013). We did not detect binding of RSPO4 to ZNRF3 in the AlphaLISA assay (this study) or using a native gel mobility shift assay (Moad and Pioszak, 2013), but the K_D of RSPO4 for ZNRF3 was reported to be 300 μM as determined by surface plasmon resonance (Zebisch et al., 2013), which is likely below the detection limit of our assays.

Our findings highlight that RSPO4 Fu1–Fu2 is in fact very potent despite its weak efficacy. We propose that the weak efficacy of RSPO4 results from its very poor ability to recruit ZNRF3 into the ternary complex with LGR4, whereas the strong potency of RSPO4 in large part results from its strong affinity for LGR4. As signaling potency reflects a complex mixture of receptor binding affinity and efficacy, the approximately equivalent potencies of RSPO4 and RSPO2/3, despite the increased LGR4 binding affinity of RSPO4, can be

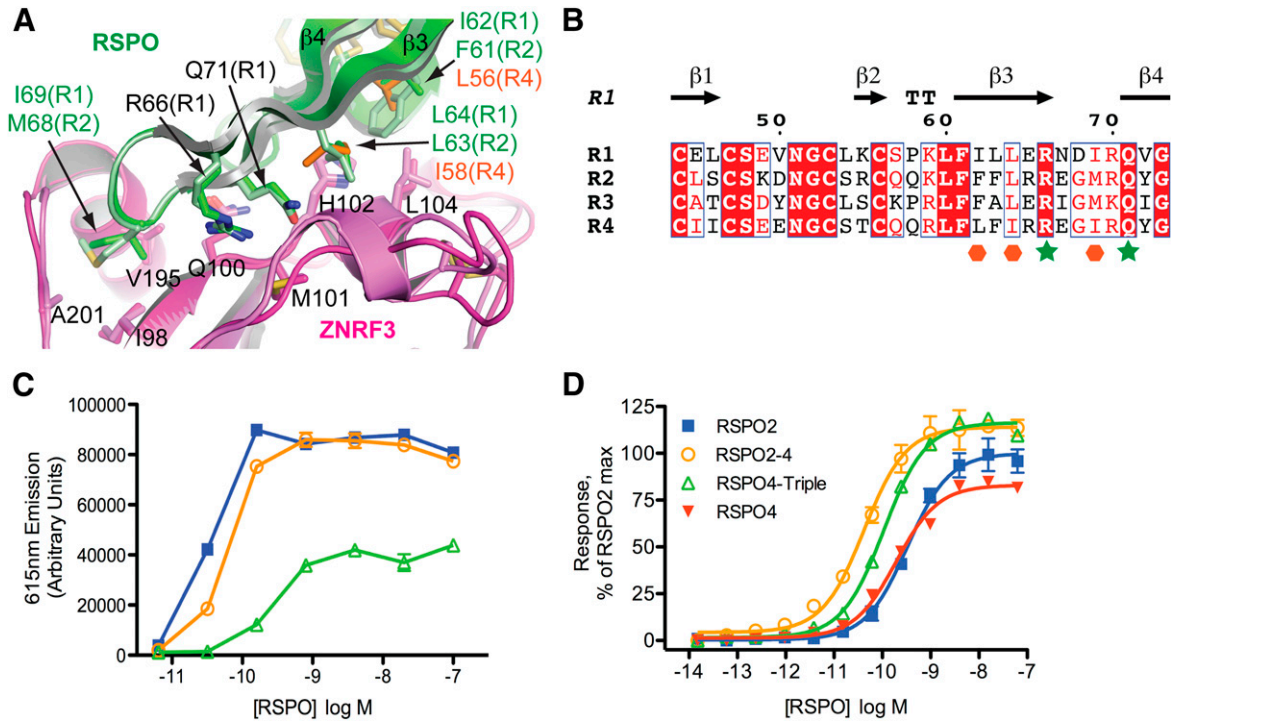

Fig. 8. Increasing RSPO4 signaling potency and efficacy with amino acid substitutions that increase affinity for ZNRF3. (A) Superimposed crystal structures of RSPO1 and -2 Fu1–Fu2 bound to ZNRF3 ECD highlighting conserved and nonconserved interactions involving the second RSPO β-hairpin. RSPO1 and -2 are dark and light green, respectively, and the ZNRF3 ECDs are shown in shades of magenta. Modeled RSPO4 residues L56 and I58 are shown in orange (PDB ID 4C9R and 4CDK). (B) Amino acid sequence alignment of the four human RSPOs for the ZNRF3/RNF43-interacting region. Conserved RSPO residues that are critical for ZNRF3/RNF43 interaction are highlighted with green stars and the variable positions in β-strand 3 that contact ZNRF3/RNF43 are highlighted with orange hexagons. (C) ZNRF3 binding AlphaLISA assay as in Fig. 2C except that donor and acceptor beads were at 15 μg/ml each. Data shown are representative of at least two independent experiments each performed in duplicate. The error bars represent the S.E.M. of the experiment. (D) TOPFLASH Wnt signaling assay with the indicated MBP-Th-RSPO Fu1–Fu2 proteins. Data shown are representative of at least four independent experiments each performed in duplicate. The error bars represent the S.E.M. of the experiment.

explained by the lower efficacy contribution of RSPO4 to its signaling potency. If ZNRF3 recruitment determines efficacy, then RSPO1 would also be expected to exhibit reduced efficacy compared with RSPO2/3 because it bound ZNRF3 relatively weakly (Fig. 2C). Although the RSPO1 maximal response was not statistically different than that of RSPO2, the trend nonetheless suggested a slightly diminished maximal response as compared with RSPO2/3 (Fig. 2E; Table 1).

The unique properties of RSPO4—having the strongest LGR4 binding but the weakest ZNRF3 binding—led us to consider combining the best binding affinity for both receptors into one RSPO molecule. We predicted that such a chimeric RSPO2–4 molecule would be a "Superspondin" with increased signaling potency due to enhanced ternary complex formation and good efficacy resulting from strong ZNRF3 recruitment, and this is precisely what we observed (Figs. 5 and 6). To further test our hypothesis, we examined the properties of a chimeric RSPO4–1 "Poorspondin" designed to combine the worst binding affinity for both receptors into one RSPO molecule. We expected that the 4–1 chimera would have weak efficacy similar to RSPO4 due to its poor recruitment of ZNRF3 and signaling potency weaker than RSPO1 due to decreased ternary complex formation. Weak efficacy similar to RSPO4 was observed for the 4–1 chimera, but its signaling potency was equivalent to RSPO1 (Fig. 7). For reasons that are unclear, the RSPO4–1 chimera retained better LGR4 binding affinity than RSPO1, which probably caused its signaling potency to be slightly stronger than predicted. Taken together, the Superspondin and Poorspondin results suggest that ternary complex formation determines RSPO signaling potency, whereas efficacy depends on ZNRF3 recruitment.

Zebisch et al. (2013) proposed that RSPO potency is determined by ZNRF3/RNF43 binding. Notably, these authors also constructed an RSPO2–4 Fu1–Fu2 chimera, but they reported that it did not have enhanced signaling activity. Enhanced signaling potency may have been missed because they used an assay based on transfection of RSPO-encoding plasmids and did not perform a full concentration-response analysis. In addition, it appears that their chimera junction point was different than ours, which may have contributed to their results. Our results are inconsistent with the idea that RSPO signaling potency is determined by ZNRF3/RNF43 binding.

To identify the structural basis for RSPOs1–4 activity differences, mutagenesis studies were performed (Fig. 8 and Supplemental Fig. 4). We sought amino acid substitutions that would confer increased ZNRF3 binding upon RSPO4 or increased LGR4 binding upon RSPO2 and thereby give rise to increased signaling potency by enhancing ternary complex formation. Introduction of three substitutions, L56F, I58L, and I63M, into RSPO4 significantly increased its ability to bind ZNRF3 and accordingly increased both signaling potency and efficacy. The RSPO4 triple mutant was not a Superspondin to the same extent as the RSPO2–4 chimera, which indicates that additional residues contribute to ZNRF3 binding affinity, perhaps in the first RSPO β-hairpin. The strong ZNRF3 binding of RSPO2/3 thus appears to partially result from the F-L-M combination at positions 62, 64, and 69 (RSPO1 numbering). Decreased RSPO1 affinity for ZNRF3 compared with RSPO2/3 may be due to I at positions 62 and 69, and I in place of L at position 64 may cause the very poor RSPO4 affinity for ZNRF3. We were less successful at engineering better LGR4 binding into RSPO2. RSPO2 [T111I] appeared to have a slight increase in LGR4 affinity and slightly increased signaling potency, but the effects were not dramatic. The molecular basis for strong RSPO4 LGR4 binding affinity may be more complex than a few different amino acid contacts with LGR4 compared with RSPOs1-3.

In conclusion, we improved our methodology for bacterial production of recombinant RSPO1–4 Fu1–Fu2 proteins to yield RSPOs with activity equivalent to those produced in eukaryotic cells and we examined the molecular basis for their differing signaling strengths. Overall, our results for the wild-type and chimeric proteins, along with the mutagenesis studies, strongly suggest that RSPO signaling potency is determined by ternary complex formation ability, whereas ZNRF3 recruitment determines efficacy. Working from this hypothesis we were able to engineer novel RSPOs with enhanced signaling potencies. The chimeric RSPO2–4 Superspondin, with 10-fold stronger signaling potency than RSPO2, may be of particular value for regenerative medicine applications or as a novel high-potency therapeutic.

Acknowledgments

The authors thank Alisha Chitrakar and Nyssa Cullin for assistance with construction of the plasmids for wild-type MBP-Th-RSPO2, -3, -4 Fu1–Fu2 expression; Drs. E. Yvonne Jones and A. Radu Aricescu for kindly providing the pHLsec plasmid; Drs. Chris West and Blaine Mooers for the suggestion to degas buffers; and Drs. Debbie Hay and Sang-Min Lee for advice on statistical analysis.

Authorship Contributions

Participated in research design: Warner, Pioszak.
Conducted experiments: Warner, Bell, Pioszak.
Performed data analysis: Warner, Pioszak.
Wrote or contributed to the writing of the manuscript: Warner, Pioszak.

References

Aoki M, Mieda M, Ikeda T, Hamada Y, Nakamura H, and Okamoto H (2007) R-spondin3 is required for mouse placental development. *Dev Biol* **301**:218–226.
Aricescu AR, Lu W, and Jones EY (2006) A time- and cost-efficient system for high-level protein production in mammalian cells. *Acta Crystallogr D Biol Crystallogr* **62**:1243–1250.
Barker N and Clevers H (2010) Leucine-rich repeat-containing G-protein-coupled receptors as markers of adult stem cells. *Gastroenterology* **138**:1681–1696.
Bell SM, Schreiner CM, Wert SE, Mucenski ML, Scott WJ, and Whitsett JA (2008) R-spondin 2 is required for normal laryngeal-tracheal, lung and limb morphogenesis. *Development* **135**:1049–1058.
Bhanja P, Saha S, Kabarriti R, Liu L, Roy-Chowdhury N, Roy-Chowdhury J, Sellers RS, Alfieri AA, and Guha C (2009) Protective role of R-spondin1, an intestinal stem cell growth factor, against radiation-induced gastrointestinal syndrome in mice. *PLoS ONE* **4**:e8014.
Blaydon DC, Ishii Y, O'Toole EA, Unsworth HC, Teh MT, Rüschendorf F, Sinclair C, Hopsu-Havu VK, Tidman N, and Moss C et al. (2006) The gene encoding R-spondin 4 (RSPO4), a secreted protein implicated in Wnt signaling, is mutated in inherited anonychia. *Nat Genet* **38**:1245–1247.
Brüchle NO, Frank J, Frank V, Senderek J, Akar A, Koc E, Rigopoulos D, van Steensel M, Zerres K, and Bergmann C (2008) RSPO4 is the major gene in autosomal-recessive anonychia and mutations cluster in the furin-like cysteine-rich domains of the Wnt signaling ligand R-spondin 4. *J Invest Dermatol* **128**: 791–796.
Carmon KS, Gong X, Lin Q, Thomas A, and Liu Q (2011) R-spondins function as ligands of the orphan receptors LGR4 and LGR5 to regulate Wnt/beta-catenin signaling. *Proc Natl Acad Sci USA* **108**:11452–11457.
Chen PH, Chen X, Lin Z, Fang D, and He X (2013) The structural basis of R-spondin recognition by LGR5 and RNF43. *Genes Dev* **27**:1345–1350.
de Lau W, Barker N, Low TY, Koo BK, Li VS, Teunissen H, Kujala P, Haegebarth A, Peters PJ, and van de Wetering M et al. (2011) Lgr5 homologues associate with Wnt receptors and mediate R-spondin signalling. *Nature* **476**:293–297.
de Lau W, Peng WC, Gros P, and Clevers H (2014) The R-spondin/Lgr5/Rnf43 module: regulator of Wnt signal strength. *Genes Dev* **28**:305–316.
de Lau WB, Snel B, and Clevers HC (2012) The R-spondin protein family. *Genome Biol* **13**:242.
Glinka A, Dolde C, Kirsch N, Huang YL, Kazanskaya O, Ingelfinger D, Boutros M, Cruciat CM, and Niehrs C (2011) LGR4 and LGR5 are R-spondin receptors mediating Wnt/β-catenin and Wnt/PCP signalling. *EMBO Rep* **12**:1055–1061.

Goujon M, McWilliam H, Li W, Valentin F, Squizzato S, Paern J, and Lopez R (2010) A new bioinformatics analysis tools framework at EMBL-EBI. *Nucleic Acids Res* **38**:W695–699.

Hao HX, Xie Y, Zhang Y, Charlat O, Oster E, Avello M, Lei H, Mickanin C, Liu D, and Ruffner H et al. (2012) ZNRF3 promotes Wnt receptor turnover in an R-spondin-sensitive manner. *Nature* **485**:195–200.

Hill HE and Pioszak AA (2013) Bacterial expression and purification of a heterodimeric adrenomedullin receptor extracellular domain complex using DsbC-assisted disulfide shuffling. *Protein Expr Purif* **88**:107–113.

Ishii Y, Wajid M, Bazzi H, Fantauzzo KA, Barber AG, Blaydon DC, Nam JS, Yoon JK, Kelsell DP, and Christiano AM (2008) Mutations in R-spondin 4 (RSPO4) underlie inherited anonychia. *J Invest Dermatol* **128**:867–870.

Jin YR and Yoon JK (2012) The R-spondin family of proteins: emerging regulators of WNT signaling. *Int J Biochem Cell Biol* **44**:2278–2287.

Kazanskaya O, Glinka A, del Barco Barrantes I, Stannek P, Niehrs C, and Wu W (2004) R-Spondin2 is a secreted activator of Wnt/beta-catenin signaling and is required for Xenopus myogenesis. *Dev Cell* **7**:525–534.

Kim KA, Kakitani M, Zhao J, Oshima T, Tang T, Binnerts M, Liu Y, Boyle B, Park E, and Emtage P et al. (2005) Mitogenic influence of human R-spondin1 on the intestinal epithelium. *Science* **309**:1256–1259.

Kim KA, Wagle M, Tran K, Zhan X, Dixon MA, Liu S, Gros D, Korver W, Yonkovich S, and Tomasevic N et al. (2008) R-Spondin family members regulate the Wnt pathway by a common mechanism. *Mol Biol Cell* **19**:2588–2596.

Kim KA, Zhao J, Andarmani S, Kakitani M, Oshima T, Binnerts ME, Abo A, Tomizuka K, and Funk WD (2006) R-Spondin proteins: a novel link to beta-catenin activation. *Cell Cycle* **5**:23–26.

Koo BK, Spit M, Jordens I, Low TY, Stange DE, van de Wetering M, van Es JH, Mohammed S, Heck AJ, and Maurice MM et al. (2012) Tumour suppressor RNF43 is a stem-cell E3 ligase that induces endocytosis of Wnt receptors. *Nature* **488**: 665–669.

Moad HE and Pioszak AA (2013) Reconstitution of R-spondin:LGR4:ZNRF3 adult stem cell growth factor signaling complexes with recombinant proteins produced in Escherichia coli. *Biochemistry* **52**:7295–7304.

Nam JS, Park E, Turcotte TJ, Palencia S, Zhan X, Lee J, Yun K, Funk WD, and Yoon JK (2007) Mouse R-spondin2 is required for apical ectodermal ridge maintenance in the hindlimb. *Dev Biol* **311**:124–135.

Ohkawara B, Glinka A, and Niehrs C (2011) Rspo3 binds syndecan 4 and induces Wnt/PCP signaling via clathrin-mediated endocytosis to promote morphogenesis. *Dev Cell* **20**:303–314.

Ootani A, Li X, Sangiorgi E, Ho QT, Ueno H, Toda S, Sugihara H, Fujimoto K, Weissman IL, and Capecchi MR et al. (2009) Sustained in vitro intestinal epithelial culture within a Wnt-dependent stem cell niche. *Nat Med* **15**:701–706.

Parma P, Radi O, Vidal V, Chaboissier MC, Dellambra E, Valentini S, Guerra L, Schedl A, and Camerino G (2006) R-spondin1 is essential in sex determination, skin differentiation and malignancy. *Nat Genet* **38**:1304–1309.

Peng WC, de Lau W, Forneris F, Granneman JC, Huch M, Clevers H, and Gros P (2013a) Structure of stem cell growth factor R-spondin 1 in complex with the ectodomain of its receptor LGR5. *Cell Reports* **3**:1885–1892.

Peng WC, de Lau W, Madoori PK, Forneris F, Granneman JC, Clevers H, and Gros P (2013b) Structures of Wnt-antagonist ZNRF3 and its complex with R-spondin 1 and implications for signaling. *PLoS ONE* **8**:e83110.

Pioszak AA, Parker NR, Gardella TJ, and Xu HE (2009) Structural basis for parathyroid hormone-related protein binding to the parathyroid hormone receptor and design of conformation-selective peptides. *J Biol Chem* **284**:28382–28391.

Robert X and Gouet P (2014) Deciphering key features in protein structures with the new ENDscript server. *Nucleic Acids Res* **42**: W320–324.

Sato T and Clevers H (2013) Growing self-organizing mini-guts from a single intestinal stem cell: mechanism and applications. *Science* **340**:1190–1194.

Sato T, Stange DE, Ferrante M, Vries RG, Van Es JH, Van den Brink S, Van Houdt WJ, Pronk A, Van Gorp J, and Siersema PD et al. (2011) Long-term expansion of epithelial organoids from human colon, adenoma, adenocarcinoma, and Barrett's epithelium. *Gastroenterology* **141**:1762–1772.

Sato T, Vries RG, Snippert HJ, van de Wetering M, Barker N, Stange DE, van Es JH, Abo A, Kujala P, and Peters PJ et al. (2009) Single Lgr5 stem cells build crypt-villus structures in vitro without a mesenchymal niche. *Nature* **459**:262–265.

Seshagiri S, Stawiski EW, Durinck S, Modrusan Z, Storm EE, Conboy CB, Chaudhuri S, Guan Y, Janakiraman V, and Jaiswal BS et al. (2012) Recurrent R-spondin fusions in colon cancer. *Nature* **488**:660–664.

Takashima S, Kadowaki M, Aoyama K, Koyama M, Oshima T, Tomizuka K, Akashi K, and Teshima T (2011) The Wnt agonist R-spondin1 regulates systemic graft-versus-host disease by protecting intestinal stem cells. *J Exp Med* **208**:285–294.

Wang D, Huang B, Zhang S, Yu X, Wu W, and Wang X (2013) Structural basis for R-spondin recognition by LGR4/5/6 receptors. *Genes Dev* **27**:1339–1344.

Xie Y, Zamponi R, Charlat O, Ramones M, Swalley S, Jiang X, Rivera D, Tschantz W, Lu B, and Quinn L et al. (2013) Interaction with both ZNRF3 and LGR4 is required for the signalling activity of R-spondin. *EMBO Rep* **14**:1120–1126.

Xu K, Xu Y, Rajashankar KR, Robev D, and Nikolov DB (2013) Crystal structures of Lgr4 and its complex with R-spondin1. *Structure* **21**:1683–1689.

Zebisch M, Xu Y, Krastev C, MacDonald BT, Chen M, Gilbert RJ, He X, and Jones EY (2013) Structural and molecular basis of ZNRF3/RNF43 transmembrane ubiquitin ligase inhibition by the Wnt agonist R-spondin. *Nat Commun* **4**:2787.

Zhao J, de Vera J, Narushima S, Beck EX, Palencia S, Shinkawa P, Kim KA, Liu Y, Levy MD, and Berg DJ et al. (2007) R-spondin1, a novel intestinotrophic mitogen, ameliorates experimental colitis in mice. *Gastroenterology* **132**:1331–1343.

Zhao J, Kim KA, De Vera J, Palencia S, Wagle M, and Abo A (2009) R-Spondin1 protects mice from chemotherapy or radiation-induced oral mucositis through the canonical Wnt/beta-catenin pathway. *Proc Natl Acad Sci USA* **106**:2331–2336.

Zhou WJ, Geng ZH, Spence JR, and Geng JG (2013) Induction of intestinal stem cells by R-spondin 1 and Slit2 augments chemoradioprotection. *Nature* **501**:107–111.

Address correspondence to: Augen A. Pioszak, Department of Biochemistry and Molecular Biology, The University of Oklahoma Health Sciences Center, 975 N.E. 10th St., Oklahoma City, OK 73104. E-mail: augen-pioszak@ouhsc.edu